Coding for spatial goals in the prelimbic/infralimbic area of the rat frontal cortex

V. Hok*, E. Save*, P. P. Lenck-Santini†, and B. Poucet*‡

*Laboratory of Neurobiology and Cognition, Université de Provence, Centre National de la Recherche Scientifique, 31 Chemin Joseph-Aiguier, 13402 Marseille Cedex 20, France; and †Department of Physiology and Pharmacology, State University of New York Downstate Medical Center, Brooklyn, NY 11203

Edited by William T. Newsome, Stanford University School of Medicine, Stanford, CA, and approved February 11, 2005 (received for review October 5, 2004)

Finding one's way in space requires a distributed neural network to support accurate spatial navigation. In the rat, this network likely includes the hippocampus and its place cells. Although such cells allow the organism to locate itself in the environment, an additional mechanism is required to specify the animal's goal. Here, we show that firing activity of neurons in medial prefrontal cortex (mPFC) reflects the motivational salience of places. We recorded mPFC neurons from rats performing a place navigation task, and found that a substantial proportion of cells in the prelimbic/infralimbic area had place fields. A much smaller proportion of cells with such properties was found in the dorsal anterior cingulate area. Furthermore, the distribution of place fields in prelimbic/infralimbic cells was not homogeneous: goal locations were overrepresented. Because such locations were spatially dissociated from rewards, we suggest that mPFC neurons might be responsible for encoding the rat's goals, a process necessary for path planning.

goal coding | place navigation | unit recording

Current evidence suggests that the hippocampus is an essential part of an integrated neural system for spatial navigation (1), largely because it contains place cells, i.e., cells that code for the animal's position in the explored space (2). A key additional part of this system would be contributed by head direction cells, found in a variety of brain structures and that code for the animal's head direction (3). However, spatial navigation is a complex process and likely requires other essential elements to be competent. Thus, most recent models postulate the existence of a distributed neural network supporting complex spatial behavior, in which a variety of functions, such as place recognition, goal localization, or path planning are thought to rely on distinctive areas (4–6).

Because there is a monosynaptic, long-term potentiation-modifiable connection between the hippocampus and the prelimbic/infralimbic (PL/IL) area of the medial prefrontal cortex (mPFC) (7, 8), a structure separately known to be involved in higher-order cognitive processes (9), it seems natural to ask whether the PL/IL area is part of the spatial navigation neural system. Previous research on the behavioral correlates of PL/IL neurons recorded from rats solving complex tasks has focused either on their working memory properties (10–13) or on their spatial firing properties in simple foraging tasks (14, 15). The latter studies, however, failed to identify neurons that fire selectively as a function of the rat's location. Because PL/IL activity might be selectively modulated only when the rat is required to navigate (i.e., to locate an unmarked goal and to move toward it), we conducted a study of the spatial correlates of PL/IL cell firing while rats were performing a place navigation task in a cylinder apparatus (16). In this task, rats had to enter an unmarked trigger zone, whose location was fixed relative to a distant cue card attached to the cylinder wall. When the rat entered the trigger zone, an overhead feeder released a single food pellet. Because pellets scattered widely after dropping, the rat had to forage around the cylinder area to retrieve a pellet. Thus, this task required the rat to make target-directed movements to an unmarked goal while preserving the undirected foraging behavior necessary for sampling unit activity everywhere in the apparatus. In addition, because reward was broadly distributed over the whole cylinder, the task made it possible to disentangle the goal value of places from their reward value: any excess firing observed at a specific location could not be the direct consequence of food reward because eating could occur anywhere.

Methods

The methods used here were similar to those used for recording hippocampal place cells (17). Accordingly, we provide only a brief description of the major steps. All procedures complied with both U.S. and French institutional guidelines.

Subjects. Long Evans black-hooded male rats (Centre d'Elevage Janvier, St.-Berthevin, France) weighing 300–350 g were housed one per cage at 20°C ± 2°C, under natural lighting conditions. They had free access to water and were food-deprived to 85% of ad lib body weight.

Apparatus. The apparatus was a gray cylinder (76 cm in diameter and 50 cm high) with a plastic floor that was wiped with alcohol between each session to prevent accumulation of uncontrolled odors. The cylinder stood at the center of an evenly lit area surrounded by opaque curtains (2.5 m in diameter and 2.5 m high). A white card attached to the wall of the cylinder covered 100° of internal arc (Fig. 1*A*). When activated, a food dispenser 2 m above the cylinder dropped 20-mg food pellets on the apparatus floor. A radio fixed to the ceiling above the cylinder was used to mask uncontrolled directional sounds. The unit recording system and all equipment necessary for controlling the experiment were located in an adjacent room.

Behavioral Procedures. Behavioral training started 6 weeks before electrode implantation. After 2 weeks of daily handling, rats were first trained to retrieve 20-mg food pellets scattered on the apparatus floor (one 15-min session for 3 days). The place preference task required rats to enter a circumscribed trigger zone and stay there for at least 2 s (16). Satisfying this condition triggered the overhead dispenser to release a single 20-mg pellet, and a correct response was recorded. Because the released pellet could end anywhere in the cylinder, the rat usually had to leave the trigger zone to find the pellet. To receive another reward, the rat had to spend at least 3 s outside the trigger zone before returning to it. The trigger zone was an unmarked 10-cm radius circle (Fig. 1*A*). Training was performed in three steps, each of which was conducted in 35-min sessions (17). In step 1, the feeder was activated each time the rat entered an 18-cm radius circle. In step 2, the rat had to stay inside the trigger zone for 2 s before

This paper was submitted directly (Track II) to the PNAS office.

Abbreviations: PL/IL, prelimbic/infralimbic; CgAd, dorsal anterior cingulate area; mPFC, medial prefrontal cortex; AP, action potential; LED, light-emitting diode.

‡To whom correspondence should be addressed. E-mail: bpoucet@up.univ-mrs.fr.

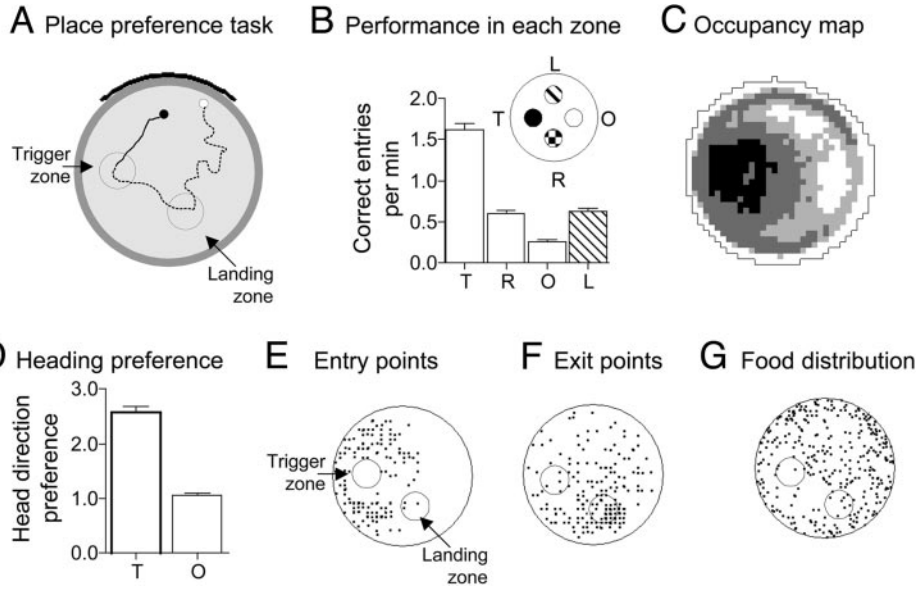

Fig. 1. Behavioral results. (*A*) A sketch of the place preference task. The rat must enter an unmarked trigger zone to release a food pellet from an overhead feeder. To eat a food pellet, the rat has to forage around the cylinder (solid line, navigation path to the trigger zone; dashed line, foraging path). In this example, the foraging path starts with an excursion into the landing zone (black dot, start of navigation path; white dot, end of foraging path). (*B*) Task performance in the trigger (T) and three control zones in adjacent right (R), opposite (O), and adjacent left (L) quadrants. (*C*) Overall occupancy map showing greater dwell times (dark pixels) in the trigger zone. (*D*) Index of heading preference toward the trigger (T) and opposite (O) zone. (*E* and *F*) Rat's positions before and after correct responses in the trigger zone used to calculate the entry and exit directions of the rat. (*G*) Food retrieval points.

a pellet was released. In step 3, the radius of the trigger zone was reduced by 1 cm per day to a final radius of 10 cm. Because previous studies found that a well trained rat makes two to three correct responses per minute (16–18), training was considered complete when the rat reached a criterion of two rewards per minute in a session. Thus, a significant fraction of time was spent by the rat foraging and eating, although behaviors not directly related to task performance (e.g., exploring or grooming) were occasionally observed.

Electrode Implantation. At the end of training, surgery to implant a driveable bundle of 10 formvar-insulated 25-μm nichrome electrodes (19) was performed under general anesthesia (pentobarbital, 40 mg/kg i.p.). The tips of the electrode bundle were implanted above either dorsal anterior cingulate area (CgAd) [3.5 mm anterior (A), 0.5 mm lateral (L) to bregma, and 2.0 mm dorsoventral (DV) to dura] or PL/IL (3.5 mm A, 0.5 mm L to bregma, and 3.5 mm DV to dura) (20).

At the completion of the experiment, the final position of the electrode array was marked by passing anodal current (15 μA for 30 s) through one of the wires. Under deep anesthesia, the rats were perfused transcardially with saline followed by 10% formalin, and their brains were removed, marked by the Prussian blue reaction, sectioned at 40-μm intervals, and stained with cresyl violet for verification of electrode placements.

Recording Methods. Beginning 1 week after surgery, the activity from each microwire was screened daily while the rat underwent additional place preference task sessions. If no waveform of sufficient amplitude was found, the electrodes were lowered 25–50 μm. Once a unit was isolated, it was recorded for a single 35-min session.

Screening and recording were done with a cable attached at one end to a commutator that allowed the rat to turn freely. The other end of the cable was connected to two colored light-emitting diodes (LEDs), a headstage with a field effect transistor amplifier (FET) for each wire and finally a connector that mated with the rat's electrode connector. The two LEDs were used for tracking the rat's head position and direction. A red LED was positioned on the midline ≈1 cm above the head and somewhat forward of the rat's eyes, whereas a green LED was set ≈5 cm behind the red LED. The FETs were used to amplify signals before they were led to the commutator through the cable. The fixed side of the commutator was connected to a distribution panel. From the panel, the desired signals were further amplified (gain: 10,000), band-pass-filtered (0.3–10 kHz), digitized (32 kHz) to be stored by a DATAWAVE DISCOVERY system (Longmont, CO). Before a recording session, spike discharges were separated by using DATAWAVE online clustering software to simplify later offline separation. The two LEDs were independently tracked with an overhead television camera connected to a digital spot follower. Each LED was detected in a grid of square regions (pixels), permitting a resolution of 6° for head direction and 2.5 cm for head position.

Data Presentation and Analysis. ***Behavioral analyses.*** For each recording session, the number of correct entries into the predefined trigger zone and three unmarked 10-cm radius circles were recorded. All four computer-defined areas were equidistant and located in the center of four equal quadrants (Fig. 1*B*). A correct entry into a given area was scored when the rat spent at least 2 s inside that area; two successive entries into an area were scored only if they were separated by at least 3 s spent elsewhere in the apparatus. A comparison of correct entries in the trigger zone (i.e., correct responses) and in the control areas provided a measure of spatial discrimination performance. To measure rat's heading behavior toward specific targets, head direction was read for each position record (excluding those during which the rat was located in the target zone), and subtracted from the target direction at the rat's current location. The time spent facing all directions relative to the target was accumulated over the entire session. Polar plots of times at all head directions (bin width = 10°) were then constructed in which heading preference for the target direction was seen as greater time in the 0° bin. Finally, an index of head direction preference was computed by dividing the time spent by the rat facing the

target direction by the average heading time across the 36 bins of the heading time distribution. Index values of >1.0 indicate a heading preference for the target location, irrespective of the rat's location in the apparatus. These calculations were done with the target being either the trigger zone or a control zone in the opposite quadrant.

Electrophysiological analyses. The first step in offline analyses was to refine boundaries for waveform clusters that were defined before recording. Candidate waveforms were discriminated by using DATAWAVE sorting software, which allows separating waveforms based on at most eight characteristic features, including spike amplitude, spike duration, maximum and minimum spike voltage, time of occurrence of maximum and minimum spike voltages, and voltage at experimenter-defined points of the waveforms. Waveforms were then processed with Plexon offline sorter (Dallas), which permits additional refinement of cluster boundaries and provide autocorrelation functions. Interspike interval histograms were built for each unit and the whole unit was removed from analysis if the autocorrelogram revealed the existence of interspike intervals <2 ms (refractory period), which is inconsistent with good isolation.

Once single units were well separated, autoscaled color-coded firing rate maps were created to visualize firing rate distributions (21). In such maps, pixels in which no spikes occurred during the whole session are displayed as yellow. The highest firing rate is coded as purple, and intermediate rates are shown as orange, red, green, and blue pixels, ranging from low to high.

A place field was defined as a set of at least nine contiguous pixels with the firing rate above the grand mean rate (21). Cells with more than two fields were discarded from further analyses. Furthermore, only the main field of cells with two fields was analyzed. The location of the field centroid was calculated according to the formula: $X_c = \Sigma x_i r_i / \Sigma r_i$ and $Y_c = \Sigma y_i r_i / \Sigma r_i$, where the coordinates X_c, Y_c of the centroid are the means of x_i and y_i (the X and Y positions of ith pixel in the field) weighted by r_i, the firing rate in the ith pixel (22). Spatial coherence, which estimates the local smoothness of place fields, was calculated as the z-transform of the correlation between the firing rate in each element of the positional firing rate array and the aggregate rate in the eight nearest pixels (23). The signal-to-noise ratio was calculated by dividing the peak firing rate averaged over the nine most active contiguous pixels in the place field by the mean firing rate over the whole apparatus.

Two methods were used to evidence possible relationships between cell discharge and the rat's speed of motion. First, a spatial map of the rat's median speed at each location in the apparatus (calculated over the session duration) was constructed by building a list of instantaneous speeds for each position record (i.e., every 20 ms). To calculate instantaneous speed, the rat's position was measured in both the current position record and 250 ms later. The speed calculated over this time interval was then assigned to the position record at the center of the 250-ms window. This calculation was repeated by sliding the window by one position record so that ultimately each position record was associated with an instantaneous speed. Rats' positions were read again so that each visited location was eventually associated with a list of instantaneous speeds. The median of the speed distribution at each location was taken as the measure of speed at that location. Based on an algorithm similar to that used for building firing rate maps, a spatial map of speeds was built and correlated with the cell's firing rate map. The cell was kept in the data set if the correlation was not significant, because the hypothesis that the place field was related one way or another to the rat's speed in the apparatus was rejected.

A second, complementary method was used to further assess significant correlations between speed and cell firing. This method was required because some locations were unavoidably associated with large variations in speed. For example, the task required the rat to stop in the trigger zone. Thus, greater cell activity in the trigger zone was necessarily associated with low speeds, resulting in a significant speed map/firing rate map correlation. To deal with this correlation, the rat's speed in other parts of the cylinder (usually, the half of the cylinder opposite to the location of the field) was measured for each 500-ms interval and plotted in 1-cm/s bins. The total number of spikes accumulated during the same periods of 500 ms was measured, and the mean firing rate for each velocity bin over the entire session was calculated. The correlation between the rat's velocity and the cell's firing rate was then calculated. The cell was discarded if this calculation yielded a significant correlation, reflecting an ambiguous spatial firing pattern.

Results

Behavior. Successful unit recordings from mPFC neurons were obtained from 10 rats that performed the task reliably in 136 recording sessions. On average, rats made 1.6 correct responses per min, a performance level that was slightly lower than during the final presurgery period ($P < 0.05$). This difference was caused by a drop in performance during early postsurgery recording sessions. It took three to eight recording sessions for the rats to recover presurgery scores. After recovery, rats scored 2.1 ± 0.1 correct responses per min on average, a performance level close to that reported in previous studies (16–18). To rule out the possibility that rats found the trigger zone by chance, we compared the rat's performance in the trigger zone and three control zones across all recording sessions (Fig. 1*B*). Rats made more correct entries in the trigger zone than in any other zone ($F_{3,136} = 159.7$, $P \ll 0.001$). All post hoc comparisons between the trigger zone and other zones yielded significant differences ($P \ll 0.001$). Based on the occupancy time maps of all recorded sessions, we built a composite time map, providing visual confirmation of the rats' highly significant preference for the trigger zone (Fig. 1*C*). Finally, the analysis of rats' heading direction revealed that rats spent more time facing the trigger zone than other directions. The index of head direction preference toward the trigger zone (Fig. 1*D*; see *Methods*) yielded a value of 2.59 ± 0.09, indicating that rats spent much more time facing the trigger zone, when away from it, than other directions. This value largely exceeds the expected value of 1.0 if there was no heading preference ($t_{135} = 18.3$, $P \ll 0.001$). In contrast, there was no head direction preference toward the opposite, control zone ($t_{135} = 1.1$ ns). In summary, rats made more entries into the trigger zone than into other zones and their heading direction pointed preferentially toward the trigger zone, indicating accurate discrimination of the trigger zone as a goal target.

Additional behavioral analyses revealed that within-session performance was stable, because no difference was found in the number of correct responses during the first and last 15 min of all recording sessions (1.62 ± 0.06 vs. 1.54 ± 0.06 correct responses; ns, not significant). Entry points in the trigger zone during correct responses were homogeneously distributed (Fig. 1*E*; $R = 0.29 \pm 0.05$; Rayleigh's test, ns), suggesting the rat did not rely on fixed paths to solve the task. In contrast, with repeated training most rats came to associate the landing zone with food delivery. Presumably, localization of the landing zone relied on auditory cues (i.e., noises produced by the pellet hitting the floor). Because the floor was cleaned between sessions, odors were unlikely to provide salient cues, but their role cannot be completely discarded. In any case, rats were observed to reliably start their foraging path by going first to the landing zone, and only then, searching for the released pellet (Fig. 1*A*). To measure this trend, we calculated for each session the rat's mean motion direction relative to the landing zone 2 s after a correct response in the trigger zone and found it to be aimed at the landing zone in all rats. For example, the mean direction averaged across the first 10 recording sessions (320 trials) for a

Table 1. Main characteristics of recorded neurons (means ± SEM)

Neurons	Mean firing rate, AP per s	Spike height, *V*	Spatial coherence
CgAd (n = 135)	1.7 ± 0.2*	164 ± 7**	0.32 ± 0.02**
PL/IL (n = 272)	2.6 ± 0.2	206 ± 6	0.38 ± 0.03

*, $P < 0.01$; **, $P < 0.0001$, compared with PL/IL.

rat whose exit points are illustrated in Fig. 1*F* deviated from the landing zone direction by only 9° ± 6° (R = 0.55 ± 0.05; Rayleigh's test, $P < 0.001$). Importantly, pellet density was not higher in the landing zone than elsewhere in the cylinder (Fig. 1*G*). Thus, both the trigger and landing zones were potential fixed goals spatially dissociable from reward finding (which could occur everywhere in the cylinder), thus allowing us to disentangle the goal value of places from their reward value.

Electrophysiological. Overall, 407 well isolated neurons were studied (mean = 2.99 ± 0.16 neurons per session). Based on histological control and reconstruction of electrode track by using the daily record of electrode position, 135 and 272 cells were recorded from the deep layers of CgAd and PL/IL, respectively (Table 1 and Fig. 2). Although PL (n = 192) and IL cells (n = 80) were initially treated separately, we finally pooled them together because their firing properties were not markedly different; in addition, both regions receive strong hippocampal projections, contrary to CgAd. Even though we were very conservative about analyzing only well separated waveforms, our recording technique does not guarantee that, on rare occasions, waveforms from two distinct cells were falsely assigned to a single cell. However, this finding does not affect our main conclusions.

Based on their spatial coherence and visual inspection of spatial firing rate maps, a substantial proportion (69 of 272, ≈25%) of cells in PL/IL regions of mPFC were found to have clear spatial correlates in the cylinder (Fig. 3*A*). Whereas spatial coherence was only 0.34 (± 0.01 SEM) for cells with no apparent place field, it was greater for the 69 PL/IL cells with a place field (mean = 0.48 ± 0.01, $P < 0.0001$, with mean signal-to-noise ratio = 3.54 ± 0.30; see *Methods*). However, spatial coherence for these cells was significantly lower than for hippocampal place cells recorded under the same conditions (0.68 ± 0.02; $P < 0.0001$) (17). In agreement with their reduced spatial coherence, the size of PL/IL place fields was much greater than for hippocampal place cells. With a firing rate cutoff set at the cell's mean discharge rate for inclusion of a pixel in a field, PL/IL field size was 146 ± 7 pixels compared with 114 ± 7 pixels for hippocampal place cells ($P < 0.01$; overall size of the cylinder was ≈725 pixels). However, with a cutoff set at 0.001 action potential (AP) per s (therefore including in the field all pixels in which at least one AP occurred), PL/IL field size was 499 ± 26 pixels compared with 149 ± 11 pixels for hippocampal place cells ($P \ll 0.0001$). These two parameters (spatial coherence and place field size) suggest a much noisier signal for PL/IL cells than for hippocampal place cells. Finally, only 6 of 135 cells (4%)

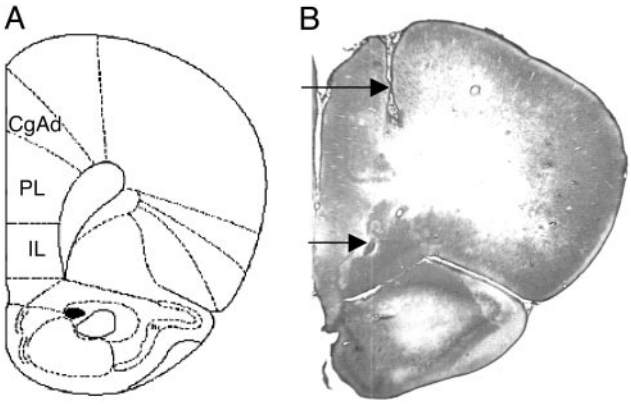

Fig. 2. Histological results. (*A*) Coronal representation of the brain showing mPFC areas (20). (*B*) Photograph of a stained section showing electrode track (top arrow) and final location of the electrode tip (bottom arrow).

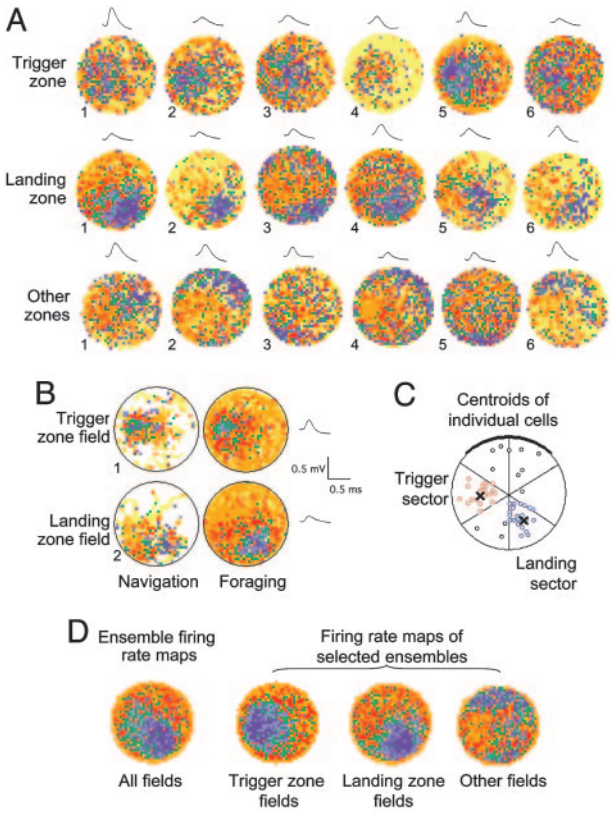

Fig. 3. Electrophysiological results. (*A*) Firing rate maps of representative cells with fields in trigger zone (top row), landing zone (middle row), or other zones (bottom row) with average waveform shown for each cell (calibration bar common to all waveforms). Each firing rate map was built by using the data from the entire recording session. In all maps, yellow indicates no firing. Color codes (median firing rates). Trigger zone cells. No. 1: orange, 0.8; red, 1.5; green, 2.3; blue, 3.1; and purple, 4.6 AP per s; no. 2: 1.7, 2.9, 3.8, 4.8, and 6.6 AP per s; no. 3: 1.3, 2.3, 3.2, 4.6,and 7.1 AP per s; no. 4: 0.6, 1.1, 1.5, 2.1, and 2.9 AP per s; no. 5: 1.7, 3.8, 5.9, 7.8, and 11.1 AP per s; no. 6: 16.3, 19.8, 22.4, 25.0,and 28.8 AP per s; Landing zone cells. No. 1: 1.2, 2.3, 3.8, 6.2, and 11.9 AP per s; no. 2: 0.4, 0.7, 1.2, 2.2, and 4.6 AP per s; no. 3: 2.2, 3.4, 4.8, 6.1, and 8.0 AP per s; no. 4: 1.7, 2.9, 3.8, 4.8,and 6.6 AP per s; no. 5: 0.5, 0.9, 1.5, 2.4, and 4.5 AP per s; no. 6: 0.3, 0.7, 1.2, 2.1, and 4.2 AP per s; Other zone cells. No. 1: 2.4, 4.4, 6.8, 10.4, and 16.7 AP per s; no. 2: 0.6, 1.2, 2.0, 3.5, and 7.1 AP per s; no. 3: 0.7, 1.2, 1.8, 2.5, and 3.9 AP per s; no. 4: 1.1, 2.1, 3.2, 4.3, and 6.6 AP per s; no. 5: 1.3, 2.1, 2.8, 3.5, and 4.9 AP per s; no. 6: 1.2, 2.0, 3.1, 4.4, and 8.3 AP per s. (*B*) Firing rate maps of trigger zone cell no. 5 and landing zone cell no. 1 broken down to separate navigation episodes from foraging episodes. Navigation maps were based on 4-s data samples taken before (trigger zone field) or after (landing zone field) correct responses. Foraging maps were constructed from remaining data samples. Despite sampling time differences, navigation maps look similar to foraging maps for both the trigger and the landing zone cells, showing that firing was not restricted to a specific type of episode (color codes as in Fig. 3*A*). (C) Spatial distribution of field centroids in the cylinder in equally sized radial sectors (X marks the centers of trigger and landing zones). (*D*) Ensemble firing rate maps calculated from all fields (n = 53), and fields in trigger zone (n = 19), landing zone (n = 22) and other zones (n = 12). See also Fig. 4, which is published as supporting information on the PNAS web site.

NEUROSCIENCE

recorded from CgAd had clear spatial correlates in the cylinder. This dissociation between CgAd and PL/IL areas is consistent with the known anatomical projections from the ventral hippocampus to PL/IL area (7, 8). Because of the rare occurrence of spatial signals in CgAd, we focused the remaining analyses only on PL/IL cells.

Because place fields can be a byproduct of heterogeneous speed profiles (e.g., lower speed in the trigger zone relative to other regions), we looked at possible relationships between a rat's speed and cell discharge (see *Methods*). Sixteen cells whose place fields could be explained by local variations in rat's speed were discarded from further consideration. The remaining 53 place fields could not be accounted for by motion-related modulations of discharge. Similarly, elevated firing in trigger or landing zones might result from specific task-related behaviors or events (such as sounds produced by feeder activation or by pellet landing) occurring in these locations. To test this hypothesis, we analyzed cell discharge in epochs temporally close to, or remote from, rewarded responses. Thus, for fields in the trigger zone, cell discharge in the field location during a 4-s period immediately before a correct response (that we called a navigation episode) was compared with the discharge in the same location during 4-s bouts of foraging (that we called a foraging episode). Discharge averaged over cells was similar for the two types of episodes (4.27 $\pm$ 1.12 AP per s vs. 4.33 $\pm$ 1.20 AP per s, not significant). The same analysis was performed for fields in the landing zone by using the 4-s period immediately after a correct response, which was compared with 4-s bouts of foraging in the same location. Again, no difference in firing was found in the two types of episodes (3.98 $\pm$ 0.79 AP per s vs. 3.73 $\pm$ 0.72 AP per s, not significant). Finally, spatial firing patterns looked very similar when navigation episodes, as defined above, were compared with random foraging episodes drawn from the same recording session (Fig. 3*B*). Thus, place fields in the trigger and landing zones do not appear to depend on the occurrence of specific task-related behaviors or external events in these two locations.

To determine the spatial distribution of the 53 place fields, we calculated the centroid of each cell's place field and plotted it onto a map of the apparatus. This analysis revealed that place fields were not homogeneously distributed (Fig. 3*C*). When each field centroid was assigned to one of six equally sized radial sectors, the number of fields near the trigger and landing zones was much greater than in any other sector (trigger, 19 of 53; landing, 22 of 53; others, 12 of 53; $\chi^2 = 47.6$, dl = 5, $P < 0.0001$). Because spatial firing of PL/IL neurons was noisy, we sought to obtain a more reliable estimate of the clustering of place fields by looking at the spatial activity of cell ensembles. We first normalized cells' positional firing rate arrays (the rate in each pixel was divided by the average rate for all pixels of a cell's rate array). Then, the normalized firing rate in each pixel was averaged across all recorded PL/IL cells with a place field. Fig. 3*D* shows the resulting firing rate maps for all 53 cells, and for selected ensembles. The overall map shows a large region of increased firing, encompassing both trigger and landing zones. Ensemble maps for fields in the trigger and landing zones (whose centroids are shown in red and blue dots in Fig. 3*C*, respectively) reveal a peak of firing centered exactly on these zones. Finally, the ensemble map for fields in other zones shows a peak of activity near the cue card location. This activation may reflect the significance of the cue card, whose location was crucial for computing the trigger zone location, and thus, for performing the task. However, that most place fields ($\approx$77%) were found in the immediate vicinity of the two fixed goal regions suggests that spatial correlates were most usually tied to the motivational salience of these specific places.

Further evidence for this conclusion is provided by the results of additional sessions that tested the effects of rotating the wall card plus trigger zone or repositioning the landing zone on landing zone fields. On four distinct occasions in which a landing zone cell was recorded, the wall card and trigger zone were rotated by 90°. Rotation of the wall card was made while the rat was away from the apparatus, and resulted in immediate rotation of the rat's search behavior (see Fig 5, which is published as supporting information on the PNAS web site). As a result, the rats looked for the trigger zone in a location consistent with the new location of the cue card. Field location was not changed, indicating that landing zone fields were independent of both the card and trigger zone. In contrast, moving the feeder above the apparatus induced rapid relocation of the field in the new landing zone, while leaving unaltered the rat's search pattern in the trigger zone. Because finding food rewards could occur anywhere in the apparatus, field relocation was not caused by food-related behavior, but more likely reflected the altered location of the landing zone.

Discussion

We recorded mPFC neurons while rats were performing a place navigation task, and found that $\approx$25% of PL/IL neurons had clear spatial correlates. This finding is remarkable because no evidence for delimited firing fields or even reliable regions of elevated firing was found when the rat had simply to forage in a cylinder (14, 15). Thus, PL/IL neurons seem much more likely to display location-specific firing when the rat is engaged in spatial navigation task than when it simply wanders about in the environment. The observation that PL/IL neurons can have behavioral correlates during complex spatial behavior is not new. Thus, PL/IL cell activity recorded from rats that solve a spatial working memory task on the radial arm maze can be strongly modulated during specific phases of the task, such as goal arrival, goal leaving, arm selection, or even food anticipation at the arm ends (10, 11). However, one difficulty of radial maze studies is that they do not allow us to separate food consumption itself from other components of the task, such as reward expectation or path selection.

The present study removed part of the difficulty because the rat's fixed goal locations were dissociated from eating locations. Thus, clustering of place fields in the immediate vicinity of the two fixed goal regions suggests that they were tied to the motivational salience of these specific places. Remaining fields were found in various locations, although marginal clustering was found near the cue card. Therefore, it is possible that PL/IL cells encode other significant aspects of the environment, such as salient landmarks or preferred locations. In addition, goal cell discharge did not appear to result from the occurrence of task-related specific behaviors. In sum, these cells appear to provide a reliable signal about the location of goals. This type of coding is consistent with models in which spatial planning relies on the activity of a prefrontal network that associates places with their motivational salience (6). In such models, goals are represented by motivational nodes. Because the PL/IL area of mPFC receives direct projections from the ventral hippocampus (7, 8), the merging of goal information with hippocampal information about the rat's current location could bias downstream areas, such as the ventral striatum, toward the selection of the motor output most relevant for reaching the goal. In conclusion, PL/IL neurons have properties expected of cells encoding spatial goals, a key component necessary for computing optimal paths in the environment (24). Although neurons with similar characteristics might exist in other brain areas, it is interesting to observe that they were found in a structure that has strong connections to the hippocampus and is separately implicated in planning (25).

How could such neurons be used for navigation? We speculate that the large and somewhat diffuse place fields observed in PL/IL cells are ideally suited to provide the ground on which

paths can be computed. That is, place fields, although centered on locations of interest, cover a broad area of decrementing activity from the center. Given the small size of the recording environment, one can therefore expect that a number of them may fire at some initial rate (>0) so that motions oriented toward the rat's current goal will result in an increase of the basal discharge, whereas motions oriented away from the goal will result in decreasing activity. Thus, a simple gradient ascent might allow the rat to reach the goal. This very simple mechanism departs considerably from complex planning, but nevertheless might be useful for orienting the rat's behavior toward adopting short and reasonably efficient paths.

Although previous research has shown that the deficit produced by mPFC lesions on allocentric spatial tasks is very mild or transient (26), subtle procedural variations have been shown to be determinant for the emergence of an impairment. For example, task difficulty is clearly an important factor (27–29). The mPFC seems also to be required for temporal organization of behavior (30, 31). Presumably, planning movements for navigating efficiently in space deeply relies on such processing. Therefore, the existence of mPFC neurons that somehow code for important spatial locations might be a key component of such a system.

Even though prefrontal cell activity could implement a simple form of path planning, more complex navigation could arise from the contribution of other brain areas. One candidate structure is of course the hippocampus and its place cells. In support of this view, accumulation of hippocampal place fields has been reported to occur near the escape platform in an annular water maze (32). However, such accumulation, was not observed in a navigation task in a dry cylinder (17). Likewise, hippocampal place fields shifted to a new location when reward was shifted to that location in a square box (33), but a similar outcome was not found in maze studies (34, 35). Thus, attempts to find nonsensory goal-related place activity have so far yielded mixed results for hippocampal place cells. Even if place cells were capable of encoding goal locations, the small size of their place fields, compared with the size of PL/IL cell fields, could make it problematic for the hippocampal network to use this information for computing optimal paths. That is, a cell firing only when the rat is actually near the goal would contribute little useful information for path planning if the rat is away from the goal. In fact, recent lesion studies suggest that place cell information might be crucial for recognition of the rat's current location, including goals (36). Despite these limitations, there are ways in which place cells might contribute path planning, albeit in a manner different from PL/IL cells. For example, recent computational studies suggest that they may permit retrieval of previously encoded efficient paths (37–40), or even finding optimal new paths to any goal location in a familiar environment (41, 42). Thus, if the hippocampus encodes goal locations, it might use this information in a different way compared with the prefrontal cortex.

In summary, goal coding likely involves the contribution of several areas working in parallel, therefore allowing space for both the hippocampus and frontal cortex to operate at different levels in the organization of spatial behavior. The observation that hippocampal place cell activity is altered after large mPFC lesions clearly suggests dynamic interactions between these two brain structures (43). Further assessment of these interactions will therefore require simultaneous recordings of mPFC cells and hippocampal place cells.

We thank J. P. Banquet, P. Gaussier, and G. S. Masson for useful discussions and H. Lucchessi for histology. This work was supported by grants from the Centre National de la Recherche Scientifique Program Cognition et Traitement de l'Information and Action Concertée Incitative Program Neurosciences Intégratives et Computationnelles.

1. O'Keefe, J. & Nadel, L. (1978) *Hippocampus as a Cognitive Map* (Clarendon, Oxford).
2. O'Keefe, J. (1976) *Exp. Neurol.* **51,** 78–109.
3. Taube, J. S. (1998) *Prog. Neurobiol.* **55,** 225–256.
4. Brown, M. A. & Sharp, P. E. (1995) *Hippocampus* **5,** 171–188.
5. Mizumori, S. J. Y., Cooper, B. G., Leutgeb, S. & Pratt, W. E. (2000) *Mol. Neurobiol.* **21,** 57–82.
6. Banquet, J. P., Gaussier, P., Quoy, M., Revel, A. & Burnod, Y. (2002) in *From Animals to Animats*, eds. Hallam, B., Floreano, D., Hallam, J., Hayes, G. & Meyer, J. A. (MIT Press, Cambridge, MA), Vol. 7, pp. 141–150.
7. Ferino, F., Thierry, A.-M. & Glowinski, J. (1987) *Exp. Brain Res.* **65,** 421–426.
8. Jay, T. M., Burette, F. & Laroche, S. (1995) *Eur. J. Neurosci.* **7,** 247–250.
9. Dalley, J. W., Cardinal, R. N. & Robbins, T. W. (2004) *Neurosci. Biobehav. Rev.* **28,** 771–784.
10. Jung, M. W., Qin, Y., McNaughton, B. L. & Barnes, C. (1998) *Cereb. Cortex* **8,** 437–450.
11. Jung, M. W., Qin, Y., Lee, D. & Mook-Jung, I. (2000) *J. Neurosci.* **20,** 6166–6172.
12. Pratt, W. E. & Mizumori, S. J. Y. (2001) *Behav. Brain Res.* **123,** 165–183.
13. Baeg, E. H., Kim, Y. B., Huh, K., Mook-Jung, I., Kim, H. T. & Jung, M. W. (2003) *Neuron* **40,** 177–188.
14. Poucet, B. (1997) *Behav. Brain Res.* **84,** 151–159.
15. Gemmell, C., Anderson, M. & O'Mara, S. M. (2002) *Behav. Brain Res.* **133,** 1–10.
16. Rossier, J., Kaminsky, Y., Schenk, F. & Bures, J. (2000) *Behav. Neurosci.* **114,** 273–284.
17. Lenck-Santini, P. P., Muller, R. U., Save, E. & Poucet, B. (2002) *J. Neurosci.* **22,** 9035–9047.
18. Zinyuk, L., Kubik, S., Kaminsky, Y., Fenton, A. A. & Bures, J. (2000) *Proc. Natl. Acad. Sci. USA* **97,** 3771–3776.
19. Kubie, J. L. (1984) *Physiol. Behav.* **32,** 115–118.
20. Paxinos, G. & Watson, C. (1986) *The Rat Brain in Stereotaxic Coordinates* (Academic, New York).
21. Muller, R. U., Kubie, J. L. & Ranck, J.B. (1987) *J. Neurosci.* **7,** 1935–1950.
22. Fenton, A. A., Csizmadia, G. & Muller, R. U. (2000) *J. Gen. Physiol.* **116,** 191–209.
23. Muller, R. U. & Kubie, J. L. (1989) *J. Neurosci.* **9,** 4101–4110.
24. Poucet, B., Lenck-Santini, P.-P., Hok, V., Save, E., Banquet, J. P., Gaussier, P. & Muller, R. U. (2004) *Rev. Neurosci.* **15,** 89–107.
25. Granon, S. & Poucet, B. (1995) *Behav. Neurosci.* **109,** 474–484.
26. De Bruin, J. P. C., Sanchez-Santed, F., Heinsbroek, R. P. W., Donker, A. & Postmes, P. (1994) *Brain Res.* **652,** 323–333.
27. Ragozzino, M. E., Adams, S. & Kesner, R. P. (1998) *Behav. Neurosci.* **112,** 293–303.
28. Granon, S., Vidal, C., Thinus-Blanc, C., Changeux, J.-P. & Poucet, B. (1994) *Behav. Neurosci.* **108,** 883–891.
29. Granon, S. & Poucet, B. (2000) *Psychobiology* **28,** 229–237.
30. Hannesson, D. K., Vacca, G., Howland, J. G. & Phillips, A. G. (2004) *Behav. Brain Res.* **153,** 273–285.
31. Fuster, J. M. (1989) *The Prefrontal Cortex: Anatomy, Physiology, and Neuropsychology of the Frontal Lobe* (Raven, New York).
32. Hollup, S. A., Molden, S., Donnett, J. G., Moser, M. B. & Moser, E. I. (2001) *J. Neurosci.* **21,** 1635–1644.
33. Breese, C. R., Hampson, R. E. & Deadwyler, S. A. (1989) *J. Neurosci.* **9,** 1097–1111.
34. Speakman, A. & O'Keefe, J. (1990) *Eur. J. Neurosci.* **2,** 544–555.
35. Lenck-Santini, P. P., Save, E. & Poucet, B. (2001) *Hippocampus* **11,** 377–390.
36. Hollup, S. A., Kjelstrup, K. G., Hoff, J., Moser, M.-B. & Moser, E. I. (2001) *J. Neurosci.* **21,** 4505–4513.
37. Blum, K. I. & Abbott, L. F. (1996) *Neural Comput.* **8,** 85–93.
38. Gerstner, W. & Abbott, L. F. (1997) *J. Comput. Neurosci.* **4,** 79–94.
39. Hasselmo, M. E., Hay, J., Ilyn, M. & Gorchetchnikov, A. (2002) *Neural Netw.* **15,** 689–707.
40. Koene, R. A., Gorchetchnikov, A., Cannon, R. C. & Hasselmo, M. E. (2003) *Neural Netw.* **16,** 577–584.
41. Burgess, N., Recce, M. & O'Keefe, J. (1994) *Neural Netw.* **7**, 1065–1081.
42. Muller, R. U., Stead, M. & Pach, J. (1996) *J. Gen. Physiol.* **107,** 663–694.
43. Kyd, R. J. & Bilkey, D. K. (2003) *Cereb. Cortex* **13,** 444–451.